Adsorption Equilibrium and Kinetics of Gasoline Vapors onto Carbon-Based Adsorbents

Ibrahim I. El-Sharkawy,[†,‡] He Jing Ming,[§] Kim Choon Ng,*[,§] Christopher Yap,[§] and Bidyut Baran Saha[†]

Interdisciplinary Graduate School of Engineering Sciences, Kyushu University, Kasuga-koen 6-1, Kasuga-shi, Fukuoka 816-8580, Japan, Mechanical Power Engineering Department, Faculty of Engineering, Mansoura University, El-Mansoura, Egypt, and Department of Mechanical Engineering, National University of Singapore, 10 Kent Ridge Crescent, Singapore 119260

Adsorption equilibrium and kinetics of gasoline vapors onto two types of carbon-based adsorbents have been experimentally investigated. The adsorbents used in this study are activated carbon (AC) of type Maxsorb III and a felt-type activated carbon fiber that is known commercially as ACF-1500. The experiments have been conducted at assorted adsorbent temperatures between (20 and 60) °C by using a thermogravimetric analyzer (TGA) unit which has an accuracy of ± 0.1 μg for the vapor uptake, and the results are logged continuously. The Dubinin–Radushkevich (D−R) equation is found to be suitable to correlate the adsorption isotherms, and the Fickian diffusion model is used to represent the adsorption kinetics. The results show that although the Maxsorb III/gasoline pair has more than twice the uptake of the ACF-1500/gasoline pair at equilibrium conditions the latter has about a 10-fold improvement in the diffusion time constant.

Introduction

In the recent years, air pollution from vehicular emissions has attracted much attention because of environmental considerations. Automobiles produce two types of emissions: (i) exhaust emissions from the byproduct of combustion such as CO, CO_2, nitrogen oxides, sulfur, and carbon particles and (ii) evaporative emissions from the evaporation of the fuel. With today's efficient exhaust emission controls and gasoline formulations, the hydrocarbons produced by evaporation of the gasoline during distribution, by vehicle refueling, and from the vehicle become significant.[1,2] Consequently, research and development efforts are needed to recover the gasoline vapors from the viewpoint of environmental protection. The recovery of gasoline vapors by an adsorption technique is one of the most promising and cost-effective methods. However, the design of such adsorption systems needs accurate data about adsorption equilibrium and adsorption kinetics for the assorted adsorbent−gasoline pair. Liu et al.[3] studied the recovery of butane, benzene, and/or heptane vapors from nitrogen using BAX-activated carbon to simulate the recovery of gasoline vapors during tank filling operations. Adsorption isotherms of gasoline vapors on activated carbon have been measured by Ryu et al.[4] using a static volume method. In this study, the authors consider gasoline as a pseudopure component, and the experimental results show that activated carbon can adsorb about 2 mol of gasoline per kilogram of activated carbon at an adsorption temperature of 20 °C. Adsorption isotherms of gasoline vapors onto dry zeolite have also been studied by Ryu et al.[5] using the Töth equation for adsorption isotherms.

* Corresponding author. E-mail: mpengkc@nus.edu.sg.
† Kyushu University.
‡ Mansoura University.
§ National University of Singapore.

A literature review indicated that there is a dearth of accurate data on the adsorption kinetics of gasoline vapors onto carbon-based adsorbents. The motivation of this paper is to conduct detailed experimental investigations of the adsorption equilibria and adsorption kinetics of gasoline vapors onto two types of carbon-based adsorbents, namely, Maxsorb III and ACF-1500 using a thermogravimetric analyzer (TGA) unit.

Experimental Section

In the present study, a TGA unit of type Chan-2121 with a precision of ± 0.1 μg is used to measure the uptake kinetics of gasoline vapors onto Maxsorb III and ACF-1500. Figure 1 shows a schematic diagram of the experimental apparatus which comprises the TGA unit, a controlled temperature evaporator, vacuum pump, MKS pressure controller, MKS-Baratron pressure sensor to measure the system pressure and a thermocouple of type K to track the temperature changes with time during the experiments. More details about the experimental apparatus have been reported in earlier publications by El-Sharkawy et al.[6] and Saha et al.[7] In the present study, however, a built-in microprocessor and a compact vortex chiller system are incorporated into the TGA unit enabling the adsorption isotherms to be studied at temperatures below room temperature. The system pressure is recorded by using a MKS-Baratron pressure sensor (type 631A). A diaphragm type vacuum pump is used to evacuate the system continuously in response to the MKS (type 651C) pressure controller to maintain a preset reaction chamber pressure. At the inlet and outlet of the reaction chamber, two porous-type stainless steel filters are installed to minimize the pressure fluctuations in the sample cell under the continuous operation of the vacuum pump.

To protect the microbalance from damage which might occur due to the chemical reaction of gasoline vapors, a small amount of low density helium gas with a constant flow rate

10.1021/je700310w CCC: $40.75
Published on Web 12/04/2007

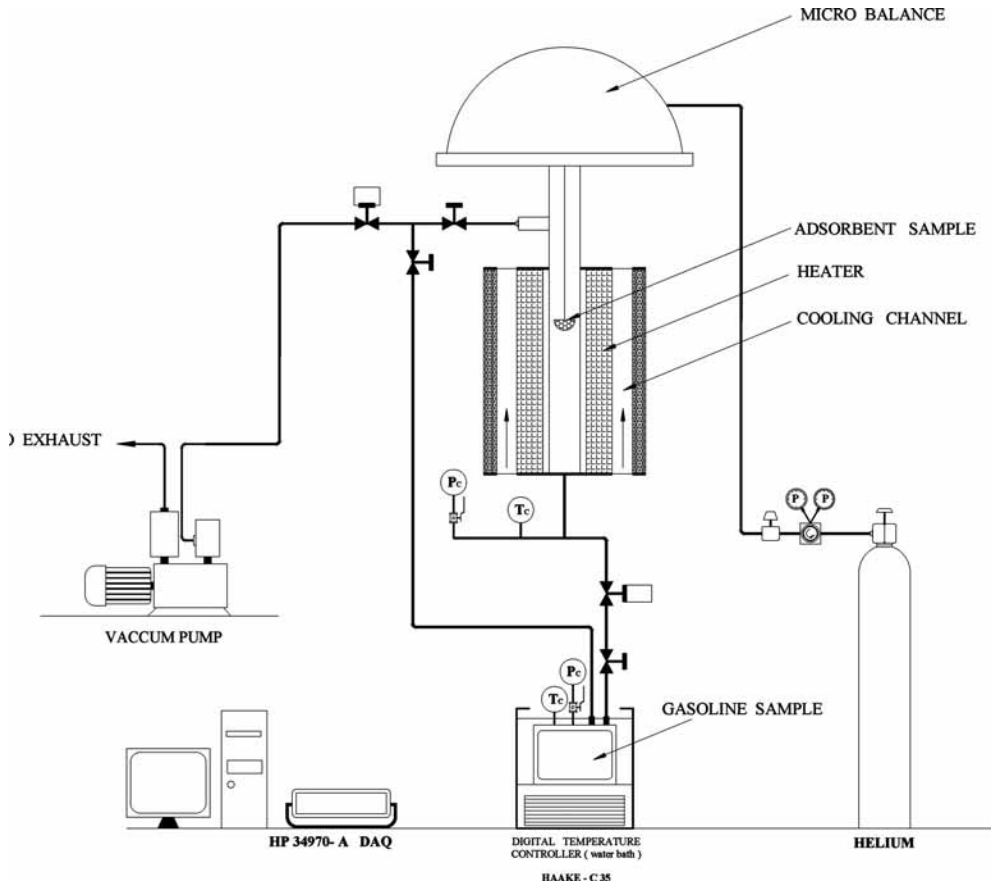

Figure 1. Schematic diagram of the experimental apparatus.

of 20 mL·min^{-1} is injected from the top of the TGA unit into the microbalance dome during the whole experiment. Gas is extracted at the top section of the TGA unit to minimize the mixing of gasoline vapor and helium gas. To avoid any condensation, an electric tape heater is mounted at the external surface of the tube connecting the evaporator and the TGA reacting chamber, maintaining the tube surface temperature at least 10 °C higher than the gasoline vapor temperature.

The adsorbent samples, typically about 87 mg of Maxsorb III and 32.5 mg of ACF-1500, are first weighed in the moisture analyzer prior to insertion into the TGA unit. It was then heated "in situ" at 140 °C for several hours. Its weight was permanently recorded to ensure that the degasification process was thorough. It was then cooled to room temperature in a dry atmosphere. After that, it was placed into the sample bowl of the TGA unit. Prior to each adsorption test, the sample was first regenerated under vacuum conditions at a temperature of 120 °C and was maintained for several hours to ensure a thorough desorption. The sample was then cooled to the required adsorption temperature until the system stabilized.

A series of adsorption experiments were carried out at different sample temperatures, namely at 20 °C, 30 °C, 40 °C, 50 °C, and 60 °C. The system pressure is kept constant at about 24 mbar where a minimum fluctuation of the system pressure is achieved. Throughout the experiments, the evaporator containing the gasoline liquid was kept constant at a temperature of 15 °C by using a constant-temperature water bath and a water circulator. The typical major components of gasoline and their corresponding volume percentage used in the present experiments are furnished in Table 1. As the assorted gasoline has many components, it is considered to behave like a pseudopure component at the evaporator temperature.

Table 1. Composition of Typical Gasoline[14]

component	value
n-paraffin	15 %
isoparaffin	30 %
cycloparaffin	12 %
aromatics	(20 to 35) %
oxygenate (max)	15 %
olefin	8 %

Table 2. Porous Characteristics of Maxsorb III and ACF-1500

adsorbent	specific surface area / $m^2 \cdot g^{-1}$	pore volume / $mL \cdot g^{-1}$	average particle diameter / μm
Maxsorb III	3140	1.70	70
ACF-1500	1300 to 1500	0.8 to 1.2	17 to 20

The porous properties of the activated carbon of type Maxsorb III, developed by the Kansai Coke & Chemicals Co., Ltd., Japan, and ACF-1500 supplied by the Tonghui Industrial & Trading Co., Ltd., China, were analyzed by using N_2 adsorption where the BET (Brunauer−Emmet−Teller) surface area and BJH (Barrett–Joyner–Halenda method) pore size distribution were experimentally investigated. The porous properties of both adsorbents are furnished in Table 2, and their photographic structures are shown in Figures 2a and 2b. The pore size distribution of the Maxsorb III is shown in Figure 2c.

Adsorption Equilibrium. A widely accepted correlation of the adsorption equilibrium of gases and vapors onto microporous adsorbents has been developed by Dubinin and co-workers from an idea originally introduced by Polanyi.[8] The theory is tested experimentally, and it is reported that it is one of the most

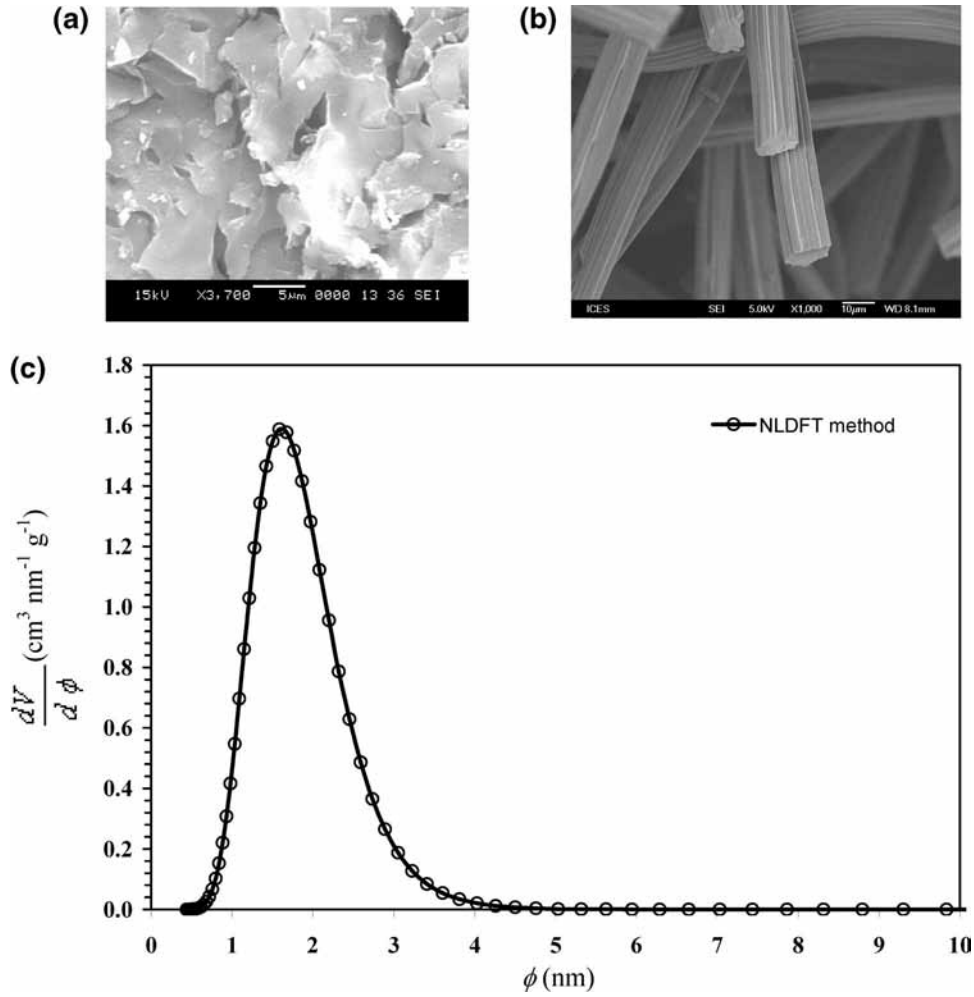

Figure 2. (a) SEM of Maxsorb III. (b) SEM of ACF-1500. (c) The pore size distribution of Maxsorb III for the nonlocal density functional theory (NLDFT) method. ϕ indicates the pore width, and $dV/d\phi$ stands for the incremental pore volume.

suitable correlations for adsorption equilibrium data for activated carbon adsorbents. Consequently, the Dubinin−Astakhov (D−A) equation (eq 1)[9] is used to fit the present experimental data of gasoline vapor adsorption onto the Maxsorb III and ACF-1500, i.e.

$$c = c_0 \exp\left\{-D\left[T \ln\left(\frac{P_s}{P}\right)\right]^n\right\} \tag{1a}$$

where $c = Wv_a$ and $c_0 = W_0 v_0$. The parameter c represents the specific volume of the adsorbate that can be adsorbed at temperature T and relative pressure P/P_s, in $m^3 \cdot kg^{-1}$. P is the equilibrium pressure, and P_s is the saturated pressure of adsorbate corresponding to the adsorption temperature. The saturated pressure of gasoline is measured experimentally and correlated as $P_s = a \cdot T_g{}^b$ where P_s is in kPa; T_g is the gasoline temperature in degree Celcius; and a and b are constants. The numerical values of a and b were estimated by least-squares regression analysis of the experimental data, and they were found to be 0.0085 and 2.31, respectively. The parameter c_0 is the total volume of micropores accessible to the given adsorbate in $m^3 \cdot kg^{-1}$. W is the mass of adsorbate per kilogram of adsorbent, and v_a is the specific volume of adsorbate in the adsorbed phase. The adsorbed phase volume cannot be measured directly, and as a consequence, its value is approximated. Generally, for adsorption at or below the adsorbate saturation temperature, it can be considered to be equivalent to the corresponding liquid specific volume. Therefore, eq 1a could be expressed as:

$$W = W_0 \exp\left\{-D\left[T \ln\left(\frac{P_s}{P}\right)\right]^n\right\} \tag{1b}$$

The parameter D is the adsorption constant that depends on the adsorbent–adsorbate pair and could be evaluated exponentially by the fitting of eq 1b. The constant n is an exponent parameter that gives the best fitting of $\ln(W)$ vs $(T \ln(P_s/P))^n$ in eq 1b. The parameter n could have any numerical value; however at $n = 2$, eq 1 is reduced to the Dubinin–Radushkevich (D−R) equation as shown in eq 2 below

$$W = W_0 \exp\left\{-D\left[T \ln\left(\frac{P_s}{P}\right)\right]^2\right\} \tag{2}$$

Adsorption Kinetics. To estimate the adsorption kinetics of gasoline vapors onto both types of adsorbents, it is essential to calculate the diffusion time constant, D_s/R^2, accurately. The semi-infinite model,[10] eq 3, provides a simple and accurate method to evaluate D_s/R^2.

$$\frac{w}{W} \approx \frac{2A}{V}\left(\frac{D_s t}{\pi}\right)^{1/2} \tag{3}$$

where A is the surface area of the adsorbent particle and V stands for the particle volume. In this study, the Maxsorb III samples are considered as spheres with radius R, whereas the ACF samples are considered as long cylinders with length L and

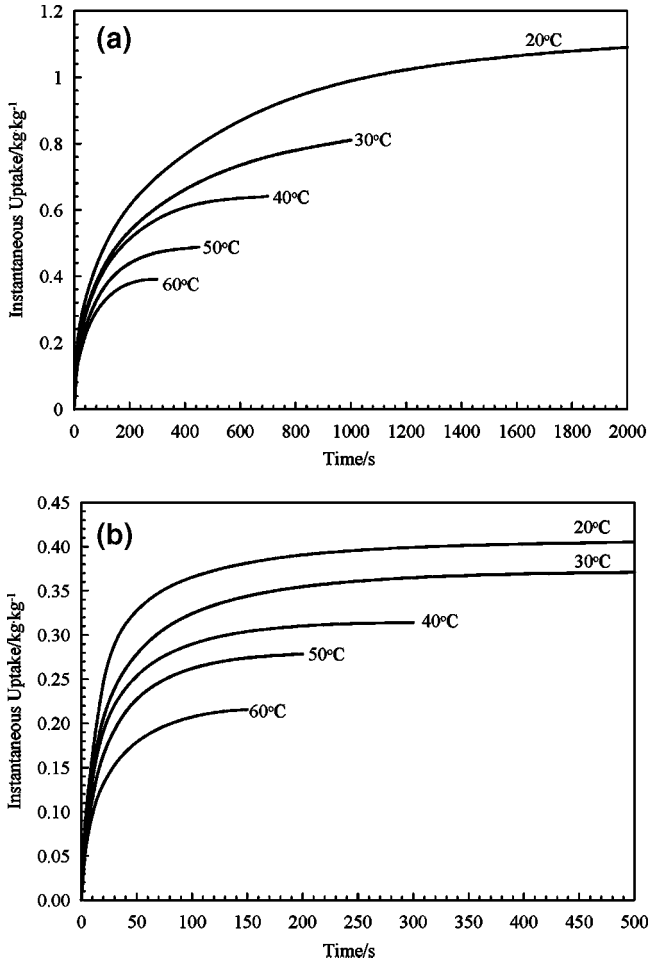

Figure 3. (a) Kinetics uptake of gasoline vapors onto Maxsorb III at assorted adsorption temperatures. (b) Kinetics uptake of gasoline vapors onto ACF-1500 at assorted adsorption temperatures.

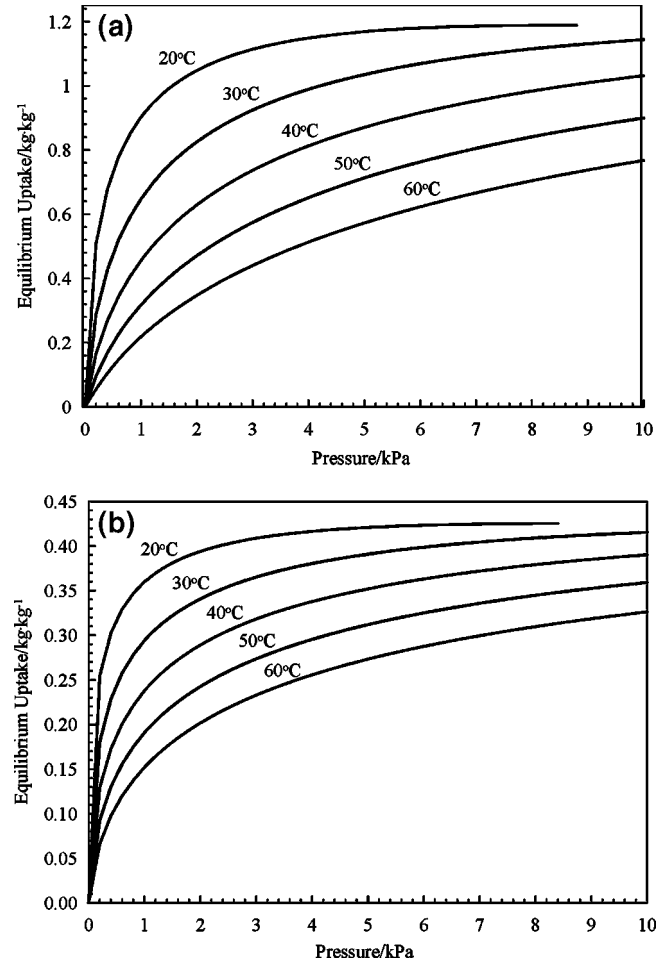

Figure 4. (a) Adsorption isotherms of gasoline vapors onto Maxsorb III as predicted by using the D−R equation. (b) Adsorption isotherms of gasoline vapors onto ACF-1500 as predicted by using the D−R equation.

Table 3. Experimental Constants of the D−R Equation

adsorbent	W_0 / kg·kg^{-1}	D / K^{-2}
Maxsorb III	1.189	$6.99 \cdot 10^{-7}$
ACF-1500	0.425	$4.244 \cdot 10^{-7}$

radius R. Owing to the small radius of ACF as compared to its length L, diffusion in the activated carbon fiber particles is considered in the radial direction only. A plot of the fractional uptake and the square root of time for each isotherm yields a straight line through the origin with a slope of $2A/V\sqrt{D_s/\pi}$.

The Fickian diffusion model is used to estimate the adsorption kinetics of different types of adsorbate pairs. Considering the shape of the spherical particle, the adsorption rate can be described by the diffusion equation (eq 4) as follows[10]

$$\frac{\partial w}{\partial t} = \frac{1}{r^2}\frac{\partial}{\partial r}\left(r^2 D_s \frac{\partial w}{\partial r}\right) \tag{4}$$

where w is the sorbate concentration; D_s is the diffusion coefficient; and r is the radial coordinate. Considering a constant diffusivity and applying the appropriate initial and boundary conditions, the solution of eq 4 can be expressed as[11]

$$\frac{w}{W} = 1 - \frac{6}{\pi^2}\sum_{n=1}^{\infty}\frac{1}{n^2}\exp\left(-\frac{n^2\pi^2 D_s t}{R^2}\right) \tag{5}$$

where n is an integer from 1 to infinity, and R is the radius of the particles. The local time-dependent concentration of a sorbate within a cylindrical ACF having a uniform micropore structure can be described by the transient diffusion equation of the form given by Crank[11] and shown by eq 6 below

$$\frac{\partial w}{\partial t} = \frac{1}{r}\frac{\partial}{\partial r}\left(r D_s \frac{\partial w}{\partial r}\right) \tag{6}$$

The solution of eq 6 can be expressed by eq 7, which is shown below[11,12]

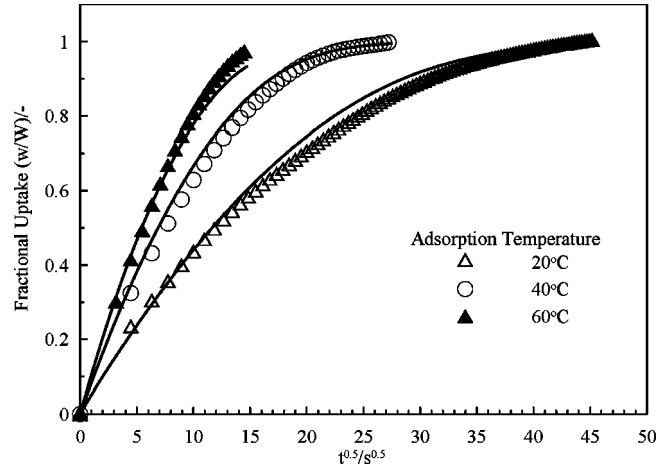

Figure 5. Plots of fractional uptake vs $\sqrt{t}$ for selected isotherms of the Maxsorb III/gasoline pair. Solid lines present eq 5, and symbols are the experimental measurements.

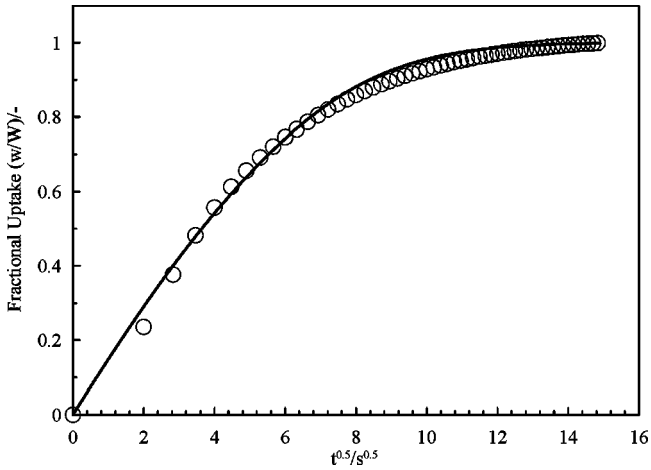

Figure 6. Plot of fractional uptake vs $\sqrt{t}$ at 40 °C for the (ACF-1500)/gasoline pair. The solid line presents eq 7, and symbols are the experimental measurements.

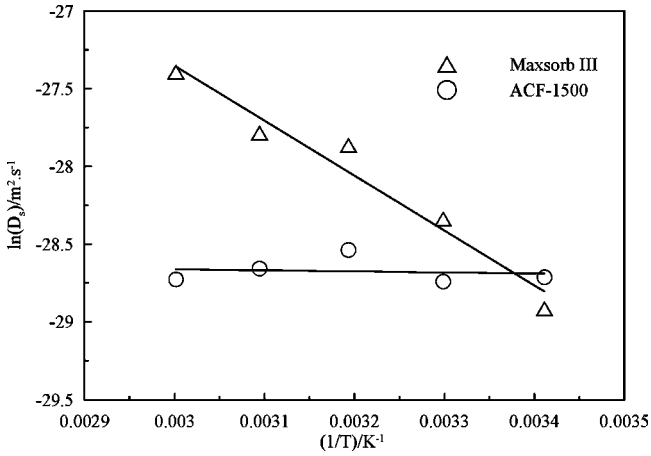

Figure 7. Variation of $\ln(D_s)$ vs $(1/T)$.

$$\frac{w}{W} = 1 - 4\sum_{n=1}^{\infty}\frac{1}{\xi_n^2}\exp\left(-\xi_n^2\frac{D_s t}{R^2}\right) \quad J_0(\xi) = 0 \qquad (7)$$

where $J_0(\xi_n)$ is the Bessel function of the first kind of order zero at various roots of ξ_n, namely, at $\xi_1 = 2.4048$, $\xi_2 = 5.5201$, and $\xi_3 = 8.6537$.

Results and Discussion

Figures 3a and 3b show the variation of uptake mass vs time for the gasoline vapor adsorption onto Maxsorb III and ACF-1500, respectively. Experiments have been carried out at five assorted adsorption temperatures in the range between (20 and 60) °C. It can be seen from Figures 3a and 3b that within an adsorption time interval of about 2000 s, the Maxsorb III can adsorb gasoline vapors as high as 1.1 kg·kg^{-1} at an adsorption temperature of 20 °C. However, only about 300 s is needed to reach the equilibrium uptake (0.39 kg·kg^{-1}) at an adsorption temperature of 60 °C. As for the ACF-1500/gasoline pair, it takes a shorter time, about 400 s, to reach the equilibrium uptake of 0.4 kg·kg^{-1} at an adsorption temperature of 20 °C. This equilibrium uptake decreases to 0.21 kg·kg^{-1} at an adsorption temperature of 60 °C which means that the Maxsorb III/gasoline pair has more than twice the uptake of the ACF-1500/gasoline pair at the same equilibrium conditions. As the uptake is measured directly by using the TGA unit, which has a precision of ± 0.1 μg, the error bars could not be seen on Figures 3a and 3b.[7]

Table 4a. Experimental Uptake of Gasoline onto Maxsorb III at 20 °C

time	w	time	w	time	w
s	kg·kg^{-1}	s	kg·kg^{-1}	s	kg·kg^{-1}
0	0.00000	680	0.90081	1360	1.04235
20	0.25068	700	0.90810	1380	1.04440
40	0.32703	720	0.91511	1400	1.04654
60	0.38403	740	0.92185	1420	1.04855
80	0.43117	760	0.92832	1440	1.05086
100	0.47161	780	0.93453	1460	1.05243
120	0.50680	800	0.94048	1480	1.05453
140	0.53773	820	0.94627	1500	1.05621
160	0.56515	840	0.95179	1520	1.05789
180	0.58973	860	0.95706	1540	1.05940
200	0.61190	880	0.96212	1560	1.06104
220	0.63203	900	0.96700	1580	1.06280
240	0.65075	920	0.97173	1600	1.06469
260	0.66818	940	0.97631	1620	1.06633
280	0.68452	960	0.98071	1640	1.06787
300	0.69985	980	0.98507	1660	1.06934
320	0.71437	1000	0.98922	1680	1.07083
340	0.72824	1020	0.99318	1700	1.07235
360	0.74154	1040	0.99689	1720	1.07384
380	0.75434	1060	1.00040	1740	1.07503
400	0.76661	1080	1.00390	1760	1.07642
420	0.77843	1100	1.00727	1780	1.07780
440	0.78997	1120	1.01044	1800	1.07919
460	0.80104	1140	1.01384	1820	1.08029
480	0.81169	1160	1.01693	1840	1.08146
500	0.82193	1180	1.01969	1860	1.08253
520	0.83191	1200	1.02258	1880	1.08384
540	0.84150	1220	1.02534	1900	1.08496
560	0.85085	1240	1.02795	1920	1.08600
580	0.85992	1260	1.03034	1940	1.08720
600	0.86872	1280	1.03307	1960	1.08830
620	0.87722	1300	1.03536	1980	1.08930
640	0.88544	1320	1.03783	2000	1.09034
660	0.89328	1340	1.04019		

Table 4b. Experimental Uptake of Gasoline onto Maxsorb III at 30 °C

time	w	time	w	time	w	time	w
s	kg·kg^{-1}	s	kg·kg^{-1}	s	kg·kg^{-1}	s	kg·kg^{-1}
0	0.00000	260	0.58164	520	0.70951	780	0.77608
20	0.20348	280	0.59492	540	0.71626	800	0.77958
40	0.28823	300	0.60745	560	0.72268	820	0.78298
60	0.33931	320	0.61929	580	0.72877	840	0.78626
80	0.38151	340	0.63054	600	0.73462	860	0.78950
100	0.41733	360	0.64120	620	0.74029	880	0.79259
120	0.44791	380	0.65133	640	0.74573	900	0.79566
140	0.47425	400	0.66091	660	0.75096	920	0.79869
160	0.49722	420	0.67003	680	0.75572	940	0.80164
180	0.51742	440	0.67869	700	0.76019	960	0.80456
200	0.53563	460	0.68694	720	0.76468	980	0.80742
220	0.55216	480	0.69487	740	0.76867	1000	0.81027
240	0.56743	500	0.70239	760	0.77244		

The Dubinin−Astakhov (D−A) equation, which is shown by eq 1b, is used to describe the experimental adsorption isotherms of both the Maxsorb III/gasoline and ACF-1500/gasoline pairs. It is found that the best fitting of the experimental data occurs when n equals 2, implying that the D−R equation (eq 2) is the most suitable correlation for the adsorption of gasoline vapors onto Maxsorb III and ACF-1500. The numerical values of W_0 and D in the D−R equation are listed in Table 3, while Figures 4a and 4b show the predicted adsorption isotherms of the Maxsorb III/gasoline and ACF/gasoline pairs using the D−R equation (eq 2). The experimental uptake data of gasoline vapors onto Maxsorb III at temperatures ranging from (20 to 60) °C are furnished in Tables 4a–e, and those for ACF-1500 are presented in Tables 5a–e.

Figure 5 shows plots of fractional uptake vs the square root of time for the Maxsorb III/gasoline vapor pair at selected

Table 4c. Experimental Uptake of Gasoline onto Maxsorb III at 40 °C

time	*w*	time	*w*	time	*w*	time	*w*
s	kg·kg^{-1}	s	kg·kg^{-1}	s	kg·kg^{-1}	s	kg·kg^{-1}
0	0.00000	180	0.49584	360	0.59536	540	0.63063
20	0.20902	200	0.51199	380	0.60167	560	0.63236
40	0.27810	220	0.52639	400	0.60727	580	0.63385
60	0.32988	240	0.53938	420	0.61215	600	0.63519
80	0.37136	260	0.55119	440	0.61642	620	0.63636
100	0.40513	280	0.56189	460	0.62015	640	0.63747
120	0.43320	300	0.57157	480	0.62341	660	0.63847
140	0.45704	320	0.58035	500	0.62622	680	0.63950
160	0.47771	340	0.58823	520	0.62862	700	0.64069

Table 4d. Experimental Uptake of Gasoline onto Maxsorb III at 50 °C

time	*w*	time	*w*	time	*w*	time	*w*
s	kg·kg^{-1}	s	kg·kg^{-1}	s	kg·kg^{-1}	s	kg·kg^{-1}
0	0.00000	140	0.39855	260	0.46158	380	0.48180
20	0.17668	160	0.41434	280	0.46690	400	0.48358
40	0.24231	180	0.42744	300	0.47126	420	0.48537
60	0.28876	200	0.43833	320	0.47478	440	0.48699
80	0.32577	220	0.44745	340	0.47760	460	0.48888
100	0.35544	240	0.45511	360	0.47989	480	0.49097

Table 4e. Experimental Uptake of Gasoline onto Maxsorb III at 60 °C

time	w	time	w	time	w	time	w
s	kg·kg^{-1}	s	kg·kg^{-1}	s	kg·kg^{-1}	s	kg·kg^{-1}
0	0.00000	80	0.29214	160	0.36127	240	0.38683
20	0.16217	100	0.31574	180	0.37061	260	0.38920
40	0.21976	120	0.33447	200	0.37774	280	0.39024
60	0.26142	140	0.34936	220	0.38308	300	0.39062

Table 5a. Experimental Uptake of Gasoline onto ACF-1500 at 20 °C

time	*w*	time	*w*	time	*w*	time	*w*
s	kg·kg^{-1}	s	kg·kg^{-1}	s	kg·kg^{-1}	s	kg·kg^{-1}
0	0.00000	130	0.37611	260	0.39665	390	0.40267
10	0.16379	140	0.37893	270	0.39733	400	0.40296
20	0.24593	150	0.38142	280	0.39798	410	0.40322
30	0.28895	160	0.38374	290	0.39859	420	0.40347
40	0.31226	170	0.38565	300	0.39910	430	0.40365
50	0.32727	180	0.38751	310	0.39965	440	0.40389
60	0.33864	190	0.38911	320	0.40016	450	0.40416
70	0.34768	200	0.39065	330	0.40055	460	0.40441
80	0.35481	210	0.39191	340	0.40092	470	0.40458
90	0.36054	220	0.39304	350	0.40132	480	0.40491
100	0.36522	230	0.39407	360	0.40167	490	0.40502
110	0.36928	240	0.39502	370	0.40203	500	0.40535
120	0.37291	250	0.39586	380	0.40234		

isotherms. In Figure 5, the solid lines represent the fitting of eq 5 where the diffusion time constant is estimated using the semi-infinite model. The goodness of the fit can be noticed in Figure 5, and thus an accurate estimation of the fractional uptake can be estimated using the Fickian diffusion model. Equation 7 provides the prediction of the fractional uptake of gasoline vapors onto ACF-1500 as shown in Figure 6 where the diffusion time constant, D_s/R^2, is estimated by using the semi-infinite model. It is found that the diffusivity of Maxsorb III increases with increases of adsorption temperature which agrees well with the Arrhenius trend as shown in Figure 7. The dependence of diffusivity on temperature is given by eq 8. However, for ACF-1500, it is noticed that the change of the diffusivity is marginal within the assorted experimental temperature range. It can also be noticed from Figure 3b that the slope of the isothermal uptake curves with time is nearly the same for long adsorption times. However, the adsorption equilibrium strongly depends on the adsorption temperature, as shown in eq 8 below

Table 5b. Experimental Uptake of Gasoline onto ACF-1500 at 30 °C

time	*w*	time	w	time	w	time	w
s	kg·kg^{-1}	s	kg·kg^{-1}	s	kg·kg^{-1}	s	kg·kg^{-1}
0	0.00000	130	0.34345	260	0.37611	390	0.38986
10	0.10851	140	0.34768	270	0.37758	400	0.39065
20	0.16379	150	0.35145	280	0.37893	410	0.39131
30	0.20902	160	0.35481	290	0.38020	420	0.39191
40	0.24593	170	0.35783	300	0.38142	430	0.39248
50	0.27171	180	0.36054	310	0.38261	440	0.39304
60	0.28895	190	0.36299	320	0.38374	450	0.39356
70	0.30226	200	0.36522	330	0.38474	460	0.39407
80	0.31226	210	0.36731	340	0.38565	470	0.39456
90	0.32044	220	0.36928	350	0.38661	480	0.39502
100	0.32727	230	0.37116	360	0.38751	490	0.39545
110	0.33332	240	0.37291	370	0.38832	500	0.39586
120	0.33864	250	0.37455	380	0.38911		

Table 5c. Experimental Uptake of Gasoline onto ACF-1500 at 40 °C

time	*w*	time	*w*	time	*w*	time	*w*
s	kg·kg^{-1}	s	kg·kg^{-1}	s	kg·kg^{-1}	s	kg·kg^{-1}
0	0.00000	80	0.27949	160	0.30554	240	0.31266
10	0.13525	90	0.28508	170	0.30691	250	0.31315
20	0.19127	100	0.28964	180	0.30817	260	0.31321
30	0.22061	110	0.29345	190	0.30926	270	0.31358
40	0.23941	120	0.29687	200	0.31020	280	0.31379
50	0.25346	130	0.29961	210	0.31110	290	0.31389
60	0.26429	140	0.30188	220	0.31163	300	0.31398
70	0.27276	150	0.30387	230	0.31216		

Table 5d. Experimental Uptake of Gasoline onto ACF-1500 at 50 °C

time	*w*	time	*w*	time	*w*	time	*w*
s	kg·kg^{-1}	s	kg·kg^{-1}	s	kg·kg^{-1}	s	kg·kg^{-1}
0	0.00000	60	0.23786	120	0.26836	180	0.27718
10	0.11502	70	0.24598	130	0.27067	190	0.27779
20	0.16448	80	0.25251	140	0.27257	200	0.27826
30	0.19257	90	0.25777	150	0.27410		
40	0.21278	100	0.26205	160	0.27535		
50	0.22723	110	0.26555	170	0.27637		

Table 5e. Experimental Uptake of Gasoline onto ACF-1500 at 60 °C

time	*w*	time	*w*	time	*w*	time	*w*
s	kg·kg^{-1}	s	kg·kg^{-1}	s	kg·kg^{-1}	s	kg·kg^{-1}
0	0.00000	50	0.17866	100	0.20716	150	0.21556
10	0.09624	60	0.18720	110	0.20994	160	0.21588
20	0.13139	70	0.19385	120	0.21210		
30	0.15266	80	0.19924	130	0.21373		
40	0.16755	90	0.20360	140	0.21484		

$$\ln(D_s) = -3.54 \cdot 10^3/T - 16.74 \quad (8)$$

Another noteworthy observation is that the diffusion time constant of the ACF-1500/gasoline pair is about 10 times larger than that of the Maxsorb III/gasoline pair because the diffusion path through the ACF is much shorter than that of granular activated carbon, assuring faster intraparticle diffusion and adsorption kinetics.[13]

Conclusions

Adsorption equilibrium and kinetics of gasoline onto activated carbon of type Maxsorb III and activated carbon fiber felt of type ACF-1500 have been successfully measured by using a thermogravimetric analyzer (TGA) unit. Experiments have been conducted within an adsorption temperature range between (20 and 60) °C. The Dubinin−Astakhov (D−A) equation was used to correlate the adsorption equilibrium. It was found that the

adsorption capacity at the equilibrium condition of the Maxsorb III/gasoline pair has more than twice the uptake as that of the ACF-1500/gasoline pair. The Fickian diffusion model was used to estimate the adsorption kinetics of both pairs. Experimental results show that the diffusion time constant of the ACF-1500/gasoline pair is about 10 times larger than that of the Maxsorb III/gasoline pair. Thus, Maxsorb III is recommended for gasoline vapor recovery for long time scale applications; however, the ACF-1500 is preferred for short time scale applications.

Literature Cited

(1) Ntziachristos, L.; Mamakos, A.; Samaras, Z.; Xanthopoulos, A; Iakovou, E. Emission control options for power two wheelers in Europe. *Atmos. Environ.* **2006**, *40*, 4547–4561.

(2) Van der Westhuisen, H.; Taylor, A. B.; Bell, A. J.; Mbarawa, M. Evaluation of evaporative emissions from gasoline powered motor vehicles under South African conditions. *Atmos. Environ.* **2004**, *38*, 2909–2916.

(3) Yujun Liu, Y.; Ritter, J. A.; Kaul, B. K. Simulation of gasoline vapor recovery by pressure swing adsorption. *Sep. Purif. Technol.* **2000**, *20*, 111–127.

(4) Ryu, Y. K.; Lee, H. J.; Yoo, H. K.; Lee, H. C. Adsorption Equilibria of Toluene and Gasoline Vapors on Activated Carbon. *J. Chem. Eng. Data* **2002**, *47*, 1222–1225.

(5) Ryu, Y. K.; Chang, J. W.; Jung, S. Y.; Lee, C. H. Adsorption Isotherms of Toluene and Gasoline Vapors on DAY Zeolite. *J. Chem. Eng. Data* **2002**, *47*, 363–366.

(6) El-Sharkawy, I. I.; Saha, B. B.; Koyama, S.; Ng, K. C. A study on the kinetics of ethanol-activated carbon fiber: theory and experiments. *Int. J. Heat Mass Transfer* **2006**, *49* (17–18), 3104–3110.

(7) Saha, B. B.; El-Sharkawy, I. I.; Chakraborty, A.; Koyama, S.; Seong-Ho Yoon, H. S.; Ng, K. C. Adsorption Rate of Ethanol on Activated Carbon Fiber. *J. Chem. Eng. Data* **2006**, *51*, 1587–1592.

(8) Polanyi, M. *Verh. Deutsch, Phys. Ges.* **1914**, *16*, 1012.

(9) Dubinin M. M. *Progress in Surface and Membrane Science*; Danielli, J. F., Ed.; Academic Press: New York, 1975; *Vol. 9*, pp l–70.

(10) Ruthven, M. D. *Principles of adsorption and adsorption processes*; John Wiley& Sons, Inc.: New York, 1984.

(11) Crank, J. *The mathematics of diffusion*, 2nd ed.; Oxford Science puplications: New York, 1975.

(12) Duong D. Do. *Adsorption analysis: Equilibria and kinetics*; Imperial College Press, 1998.

(13) Suzuki, M. Activated carbon fiber: fundamentals and applications. *Carbon* **1994**, *32* (4), 577–586.

(14) He, J. M. Adsorption Evaporative Emission Control System for Vehicle, Report of Mechanical Engineering Department, National University of Singapore, Report No. HT050329B, **2006**.

Received for review May 31, 2007. Accepted October 27, 2007.

JE700310W